May 30th, 1:45 PM - 2:00 PM

Capacity of street inlets with partially severed grate openings

S. Kemper
University of Wuppertal

A. Schlenkhoff
University of Wuppertal

DOI:10.15142/T3W01S

Capacity of street inlets with partially severed grate openings

S. Kemper[1], A. Schlenkhoff[1]
[1]School of Architecture and Civil Engineering
University of Wuppertal
Wuppertal, Germany
E-mail: s.kemper@uni-wuppertal.de

ABSTRACT

Due to an increasing number of extreme rainfall events, the management of urban flooding requires new design approaches concerning the underground drainage system as well as the temporary surface water runoff. Latest developments on bidirectional coupled models, 1D-1D as well as 1D-2D models, are already employed in practice. Street inlets are the connecting elements between the surface and the underground system. Depending on the longitudinal and transversal slope of the street as well as the street inlet type, the hydraulic efficiency of grate inlets is hardly available. Thus, physical model test runs were done. With longitudinal slopes up to 10 % only supercritical flow conditions with flow depths up to 3 cm and flow velocities of approximately 1-2 m/s occur. In previous physical model test runs the overall grate capacity of selected grate inlets was measured. Depending on the street geometry up to 75 % of the approaching surface flow is captured by the inlet. The aim of the present paper is to investigate the inflow conditions in detail. By measuring the intercepted flow for defined parts of the grate openings separately the main inflow regions with their respective efficiency can be determined. A typical street inlet used in Germany is investigated exemplarily. The main inflow areas of the grate inlet are located in a typical triangular pattern on the curbside. The front half of the inlet intercepts nearly 70 % up to 95 % of the total captured flow. Physical model results are compared to numerical results in order to calibrate and validate the numerical model. Within both models nearly the same inflow zones can be identified qualitatively.

Keywords: *street inlets, inlet capacity, supercritical flow, urban flooding*

1. INTRODUCTION

According to the Synthesis Report of the Intergovernmental Panel on Climate Change (IPCC) the number of heavy rainfall events and their intensity will increase in the future (IPCC 2014). Therefore, urban flood risk management becomes more important and requires new design approaches in urban drainage engineering. Digman et al. (2014) define four key events regarding the management of urban flooding: (1) everyday rainfall, (2) drainage design rainfall, (3) exceedance rainfall and (4) extreme rainfall. Usually, urban drainage systems are designed for events one and two with return periods of 2-10 years (DIN EN 752 2008) and consist of underground infrastructures. Street inlets capture the surface runoff and the connecting pipes then carry the discharge to the underground-piped drainage system. It is not sustainable to enlarge the underground infrastructures when designing for exceedance (key event 3). Drainage systems above the ground need to be developed to manage surface flooding e.g. flood routes or temporary storage areas. Emergency plans must exist for the case of key event four (Digman et al. 2014). According to Fratini et al. (2012) a "dual drainage" or "major and minor systems" approach has not yet been prevailed in Europe whereas e.g. in Australia the runoff after heavy rainfall events may be discharged above ground already. With bidirectional coupled numerical models the interaction between the underground drainage system (minor system) as well as the surface runoff using topography and streets (major system) can be calculated. Even extreme flow conditions can be represented (Butler and Davies 2011). 1D-1D models (one-dimensional pipe flow model and one-dimensional surface flow model) are applicable as long as the surface flow stays within the road cross-section. 1D-2D models (one-dimensional pipe flow model and two-dimensional surface flow model) give results that are more realistic if the surface flow exceeds the capacity of the street profile. Inundation areas with flow depths and velocities are calculated. Most of the coupled numerical models use a weir or orifice equation to calculate the exchange between both systems. Djordjevic et al. 2013 pointed out that uncertainties regarding the parameters exist and the equations are not fully representative of the real flow conditions. More realistic information concerning the hydraulic efficiency and flow conditions of existing street inlets is necessary to build up the bidirectional coupled numerical models. Djordjevic et al. (2013) investigated the interaction between above and below ground drainage systems with full-scale physical and three-dimensional numerical models. The authors

identified the need for a better understanding of the interaction process between above and below ground drainage systems. The authors' CFD model was able to replicate qualitatively the observed complex flow conditions in the entire street inlet system.

Street inlets exist in four types: (a) grate inlets, (b) curb-opening inlets (c) combination inlets and (d) slotted drain inlets (Brown et al. 2009), see Figure 1. The hydraulic efficiency of grate inlets depends primarily on the street's geometry with longitudinal and transverse slope, the surface runoff (discharge) and the grate itself (type, geometry, opening area). Several investigations deal with the hydraulic efficiency of grate inlets, or more precisely, only with the grates efficiency neglecting the system below, e.g. Spaliviero et al. (2000), Despotovic et al. (2005), Gómez and Russo (2005) and Guo and MacKenzie (2012).

Gómez and Russo (2007) and Gómez and Russo (2009) studied different inlet types like continuous transverse grates and macro grate inlets. Russo et al. (2013) tested methods to estimate the efficiency of non-tested continuous transverse grates. Lopes et al. (2016) investigated the ability of a volume of fluid (VOF) model to reproduce the efficiency of a continuous transverse grate inlet by comparing the results with experimental data. The authors recommend the use of a numerical model as a useful alternative to experiments to predict efficiencies of different types of inlet structures with grates, since similar results were obtained.

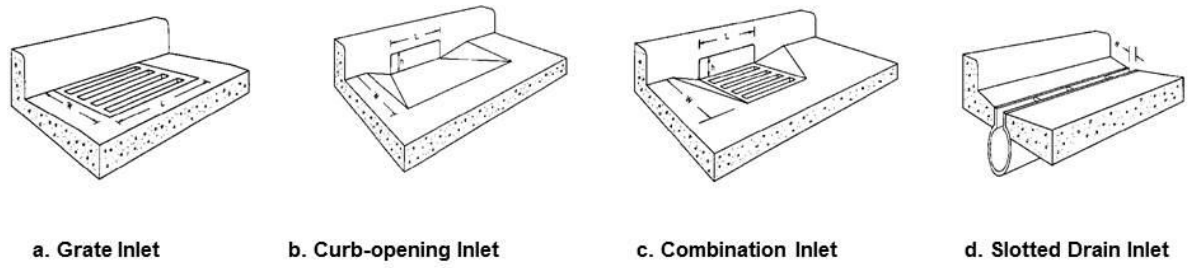

Figure 1. Street inlet types (Brown et al. 2009), modified.

There is only less information about the inflow conditions of grate inlets in detail. Detecting the discharge through defined parts of the grate openings enables for instance the prediction of a reduced efficiency due to clogging effects. Furthermore, the geometry of the grate may be improved to increase the efficiency in future research work. The present paper focuses on the main inflow areas of a grate typically used in Germany and their corresponding efficiencies.

In order to calibrate and validate a numerical model to calculate the capacity of grate inlets with an extended range of parameters, e.g. transverse slope or inlet geometry, the physical model results were compared to the numerical results.

2. MODEL SETUP

2.1. Physical Model

The physical model consists of a flume made of acrylic glass with L_{Flume} = 10.0 m in length and W_{Flume} = 1.5 m in width where the slope is adjustable in longitudinal and transverse direction. The bottom roughness is approximately k = 1.5 mm (roofing paper). In an opening area of 500 mm x 500 mm the grate of real street inlets can be integrated (scale: 1:1). All of the presented investigations were done with the standardized grate inlet mostly used in Germany and described in DIN 19583 (2012). Water depths were measured with ultrasonic sensors upstream of the inlet where steady as well as uniform flow conditions were already reached. The resolution of the ultrasonic sensors is 0.18 mm with a reproducibility of ± 0.15 % (General Acoustics e.K.). The surface flow velocities were measured with a radar measuring device with an accuracy of ± 0.5 % ± 0.03 m/s and a measuring range of 0.15 m/s up to 9 m/s (FLOW-TRONIC S.A./N.V.). Both measurements were done over the whole cross section 1 m upstream of the inlet with steps of Δy = 6 cm. Using platform load cells, the volume of the water intercepted by the grate, flowing beside the grate and flowing over the grate was measured over time. Backwater effects caused by the underground drainage system were not considered within the

presented investigations. Instead, a free outflow through the grate exists. Furthermore, only supercritical flow conditions occur for all investigated discharges and slopes and therefore no influence arises due to the physical outflow condition. In order to locate the main inflow areas of the grate, the grate was separated into eight parts (see Figure 2, right side). In addition to the described flows above, the discharge through each part was measured separately. The opening area of the grate in total is A_0 = 910.00 cm². Parts one, four, five and eight each have an opening area of $A_{1,4,5,8}$ = 97.50 cm² (10.71 % of A_0) and parts two, three, six and seven each have an opening area of $A_{2,3,6,7}$ = 130.00 cm² (14.3 % of A_0), see Table 1.

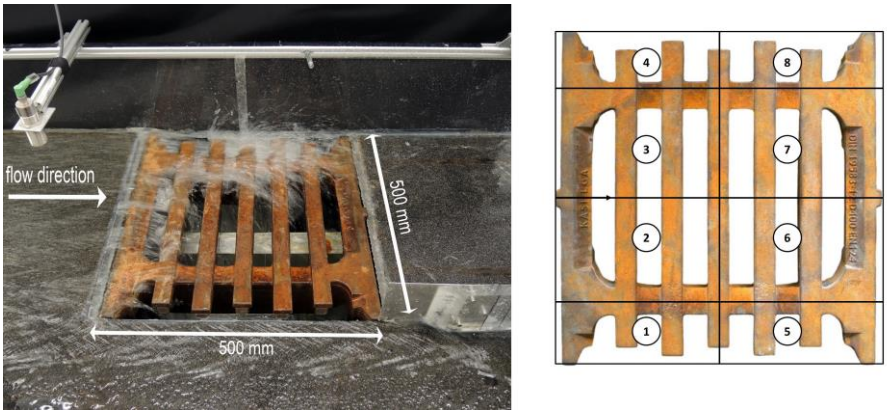

Figure 2. Detail of the physical model (left) and definition of the opening parts (right)

Table 1. Dimensions of the opening parts

Part No.	**Width b_i [cm]**	**Opening Area A_i [cm²]**	**Ratio A_i/ A_0**
1	9.8	97.50	0.1071
2	15.0	130.00	0.1429
3	15.0	130.00	0.1429
4	9.8	97.50	0.1071
5	9.8	97.50	0.1071
6	15.0	130.00	0.1429
7	15.0	130.00	0.1429
8	9.8	97.50	0.1071
Total	-	**A_0 = 910.00**	-

The German guideline for designing street inlets recommends a connected catchment area of 400 m² for one inlet each (FGSV 2005). Therefore, based on KOSTRA-DWD-2000 (2000), the surface runoff approaching one inlet can be determined assuming 100 % runoff on the street. Table 2 gives the surface runoff for Wuppertal, a city in the western part of Germany with different return periods T [a] and durations D [min] as an example.

Table 2. Surface runoff approaching one street inlet (FGSV (2005), KOSTRA-DWD-2000 (2000))

***T* [a]**	**0.5**	**1.0**	**2.0**	**5.0**	**10.0**	**20.0**	**50.0**	**100.0**
***D* [min]**	Q [l/s]	Q [l/s]	Q [l/s]	Q [l/s]	Q [l/s]	Q [l/s]	Q [l/s]	Q [l/s]
5	4.30	6.80	**9.29**	12.59	15.08	17.58	20.88	23.37
10	3.84	5.46	7.07	**9.21**	10.82	12.44	14.58	16.20
15	3.30	4.56	5.81	7.47	**8.72**	9.98	11.64	12.89

Usually, drainage structures are designed for rainfall events with T = 2 a to 10 a. In order to consider exceedance rainfall events with return periods of more than T = 10 a, the discharge for the model test runs was varied between Q = 3 l/s up to Q = 21 l/s, which corresponds to a rainfall event with T = 100 a (see Table 2). The transverse slope was fixed to S_T = 2.5 % and the longitudinal slope was varied between S_L = 2.5 % and S_L = 10.0 % with ΔS_L = 2.5 %. The present paper focuses on rainfall events with a resulting surface runoff of Q = 9 l/s (just reaching exceedance) and an intermediate longitudinal slope of S_L = 5.0 % and S_L = 7.5 %.

2.2. Numerical Model

The CFD Software FLOW-3D v.11.1 (Flow Science Inc.) was used for the numerical simulations. The model geometry was taken from the physical model, hence, no scaling effects occur. Surface tension is not calculated within the numerical model test runs. The grate inlet geometry is included using an STL (Stereo Lithography) file. The cross bar width of the grate is 32 mm and the opening width between two cross bars is 36 mm. Due to these small dimensions, the mesh size was set to $dx = dy = 4$ mm and $dz = 3$ mm in Mesh Block 2 (nested mesh block including the street inlet, see Figure 3). The mesh size of the basic mesh block 1 in z-direction corresponds to the respective parameter in mesh block 2 with $dz = 3$ mm. The mesh size in x-y direction lies between $dx = dy = 12 - 8$ mm. Previous investigations have proven the independence of the mesh. The mesh size was decreased as well as increased for *dx*, *dy* and *dz*. Convergence was reached with the resulting mesh size. The street inlet geometry was modeled precisely using the FAVOR™ method (Fractional Area-Volume Obstacle Representation, Flow Science Inc. (2015)). The numerical model consists of approximately 26 million cells in total. The RNG turbulence model was used (Renormalized group, based on the *k-ε* turbulence model). The inflow boundary condition was set to *Volume Flow Rate*, the *Outflow* condition was set for the lower boundary as well as for the outflow of the street inlet (*Zmin*). The surface roughness of the flume is $k = 1.5$ mm, the roughness of the inlet $k_I = 0.3$ mm. The discharge through each of the eight parts can be determined by defining eight plane *Baffles* as a flux surface (100 % porous, does not affect the flow*)* beneath the grate inlet. Furthermore *Baffles* were defined to measure the approaching flow as well as the water flowing beside and over the grate (see Figure 3).

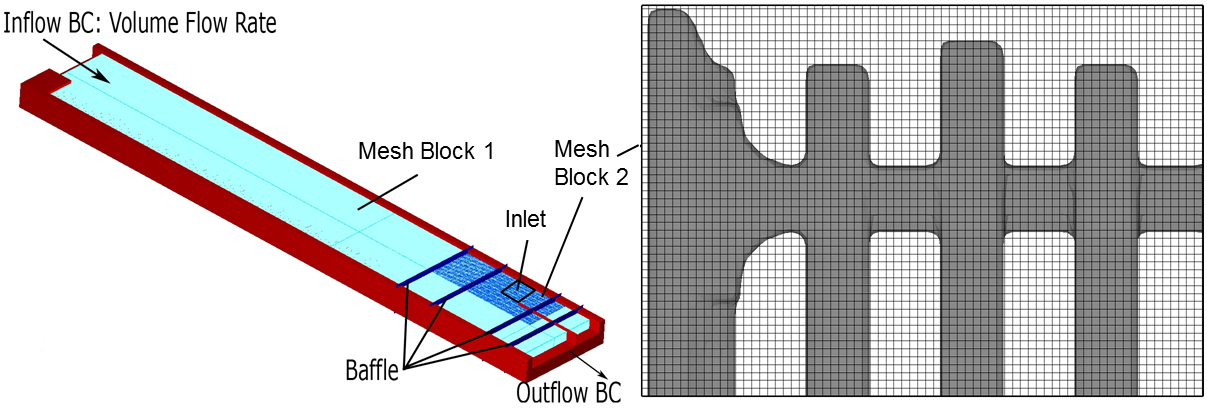

Figure 3. Numerical model

3. RESULTS AND DISCUSSION

The approaching flow is characterized by a uniform triangular cross section area with transverse slope S_T [m/m], water depth h [m] directly at the curb and water spread width W [m]. As investigated in previous test runs (Kemper and Schlenkhoff 2015) the discharge in a triangular channel can be calculated by a modified form of the Manning equation developed by Izzard (1946):

$$Q = 0.376/n \; S_T^{5/3} \; W^{8/3} \; S_L^{1/2} \qquad (1)$$

where Q = street discharge [m³/s] (approaching flow), n = Manning's roughness coefficient of the street surface [s/m$^{1/3}$], S_L = street longitudinal slope [m/m] and W = water spread width W [m] with $W = h/S_T$. The measured water depths in the laboratory, the resulting water depths from the numerical model as well as the calculated water depths from Eq. (1) are compared in Figure 4 (left). The Manning's roughness coefficient in Eq. (1) is set to $n = 0.013$ s/m$^{1/3}$. With Eq. (1) the water depths h [m] can be calculated very well – a good approach is given. Also, the numerical model results fit to the physical model results with maximum deviations of ± 10 % (Figure 4, right).

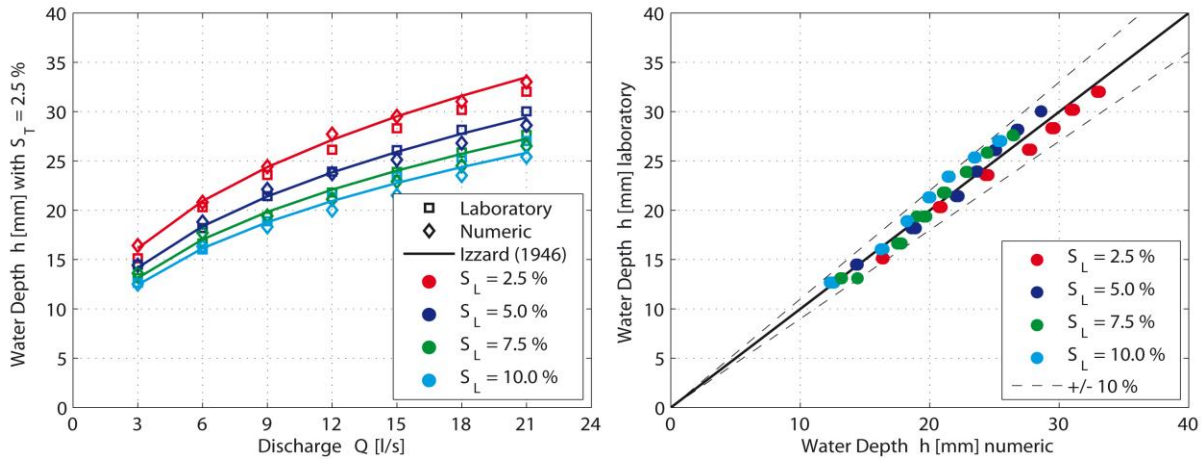

Figure 4. Water depths *h* (a) calculated with equation (1) compared to results from numerical model and laboratory and (b) corresponding comparison of water depths from numerical model and laboratory

The flow velocity upstream of the inlet measured at several points transverse to the flow direction is given for S_L = 5.0 % and S_T = 2.5 % and an exemplary approaching discharge of Q = 9 l/s in Figure 5. The velocities calculated with the numerical model differ from the physical model results with maximum deviations of ± 15 %. Uncertainties appear in the laboratory results at the transition between dry and wet areas where small velocities occur which cannot be measured with the used technique. For all test runs supercritical flow conditions appear with water depths up to 3 cm and flow velocities of approximately 1-2 m/s.

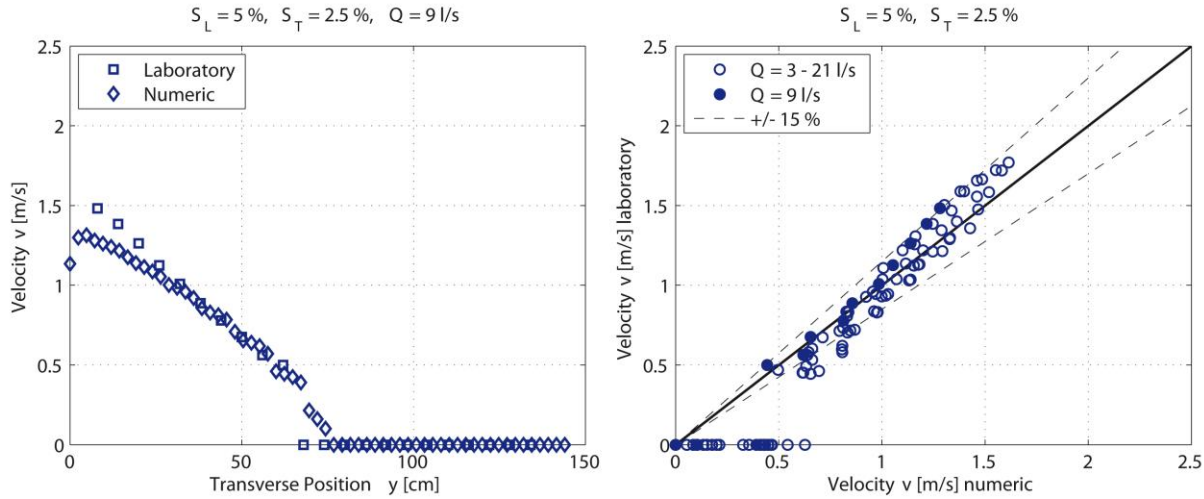

Figure 5. Flow velocities *v* (a) along cross section from numerical and physical model and (b) corresponding comparison of velocities from numerical model and laboratory

The grate capacity is defined as the quantity of the intercepted flow rate Q_I [l/s] whereas the hydraulic efficiency E of the grate inlet is described as a percentage of the approaching flow rate with:

$$E = Q_I / Q \tag{2}$$

where Q_I [l/s] is the intercepted flow rate and Q [l/s] the approaching flow. The remaining discharge $Q - Q_I$ is divided into the water flowing beside the inlet Q_B (bypass flow) and the water flowing over the inlet Q_O.

In Figure 6 the physical model results for the overall grate capacity are given with a resulting dependency curve. The total intercepted flow Q_I depends on the approaching surface flow Q. With a constant transverse slope of S_T = 2.5 % the intercepted flow rates vary between $Q_I \approx$ 2.95 l/s and $Q_I \approx$ 16.00 l/s for the investigated grate geometry, depending on the longitudinal slope and surface runoff. Therefore, the grate efficiency is minimum E = 75 %. It is expected that with increasing surface runoff the intercepted flow will converge to a maximum

value (not tested yet). The influence of the longitudinal slope is very low (Figure 6). High longitudinal slopes such as S_L = 10 % result in high flow velocities and small water spread widths on the street. The bypass flow Q_B decreases. However, the higher the flow velocities, the more water is flowing over the inlet, Q_o increases. Both effects nearly cancel each other out, then, the total amount of the intercepted flow is nearly unaffected by the longitudinal slope.

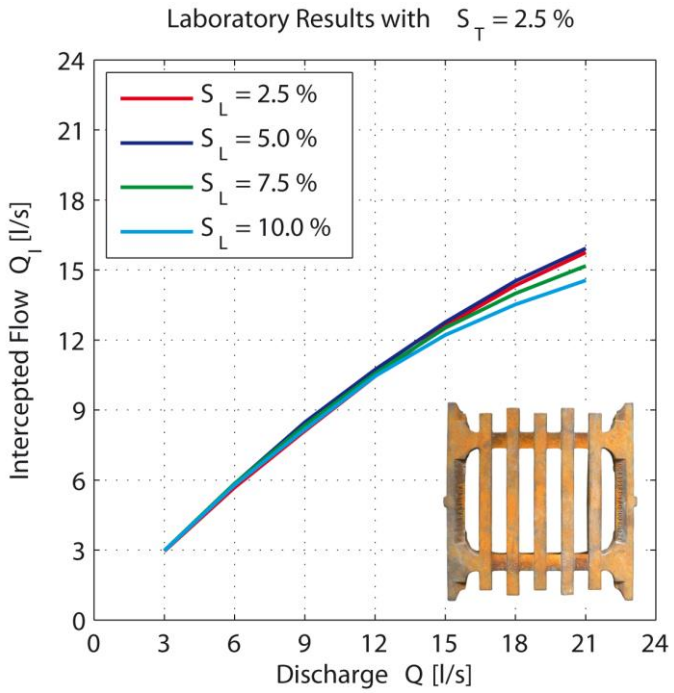

Figure 6. Intercepted flow depending on approaching flow rate (physical model results)

The efficiency of particular areas of the grate inlet can be calculated by:

$$E_i = Q_{Ii} / Q_I \tag{3}$$

Depending on the approaching flow, the front half of the inlet captures nearly 70 % up to 95 % of the intercepted water Q_I. Dividing the grate into two parts longitudinal to the flow direction, the curbside half has an efficiency of approximately 60 % up to 80 %. Referring to the division into eight parts (Figure 2, right side), the roadside back parts five and six are nearly useless. To get more detailed information about the efficiency of particular parts, the intercepted flow rate Q_I is divided into eight parts – Q_{Ii} [l/s] with i = 1, 2 … 8. Due to different opening areas $A_{0,i}$ of each part (Table 1), the specific discharge q_i is calculated with regard to the width of the part perpendicular to the flow direction b_i to achieve comparability:

$$q_i = Q_{Ii} / b_i \tag{4}$$

Two main capacity zones can be identified in Figure 7, exemplarily for longitudinal slopes of S_L = 5.0 % and S_L = 7.5 %. The front half parts of the inlet (except part one) show nearly the same capacity curve progression, as well as the remaining parts one, five, six, seven and eight. The specific discharge in the front half part can be approximated with a less than linear shape curve whereas the capacity curve progression for the back half part depends nearly linearly on the approaching flow.

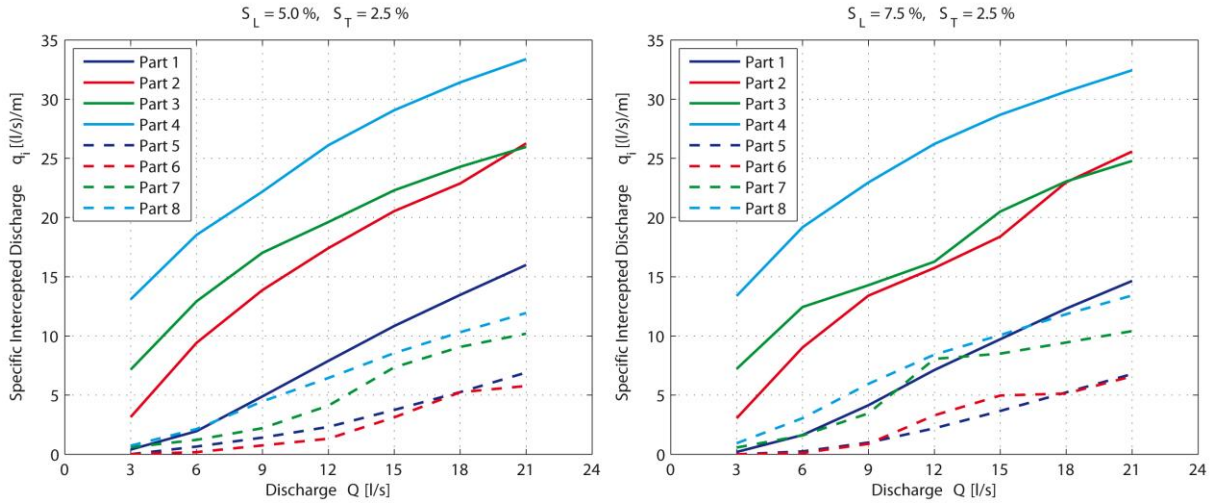

Figure 7. Specific inlet capacity (laboratory results)

Figure 8 gives interpolated specific discharges over the inlet area. The left side shows the laboratory results, the right the results from the numerical model. Flow direction is from left to right with the curbside on the upper edge.

In Table 3 the approaching flow $Q_{apr,i}$ for each transverse part is given, calculated with the measured water depths and flow velocities from both models. The corresponding intercepted flow through each part resulting from the model runs is presented in column 3. The influence of the transverse slope is recognizable since the discharge through the roadside parts is slightly higher than the approaching flow. This is caused by the additional lateral inflow from the street. Within both the laboratory and numerical model, nearly the same inflow zones can be identified qualitatively on the front curbside zone. However, the amount of the discharge still differs. Further research is necessary to investigate the ability of the used numerical model to calculate the intercepted flow rates.

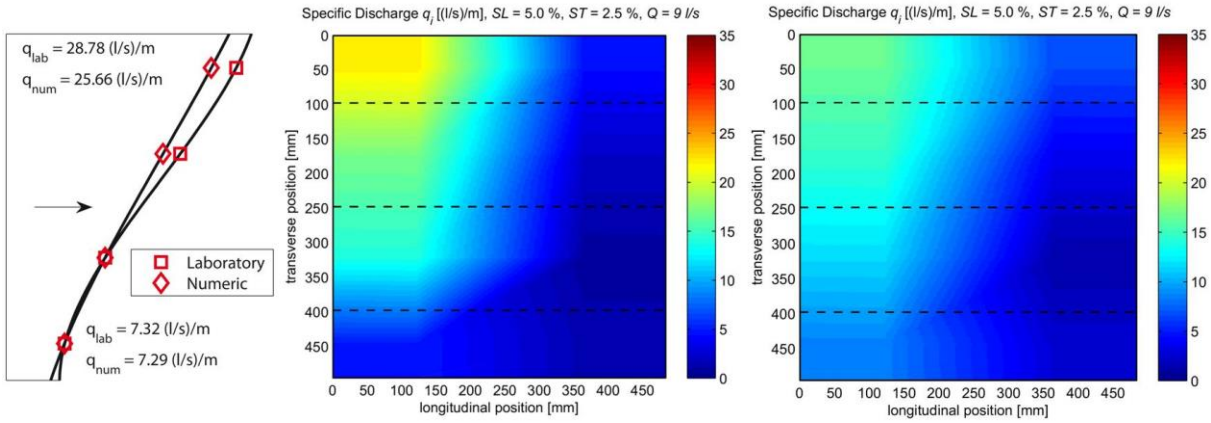

Figure 8. Specific inlet capacity – laboratory (left) vs. numeric (right), flow direction: left to right

Table 3. Approaching flow $Q_{apr,i}$ for each part with corresponding intercepted flow Q_{Ii} (Q = 9 l/s, S_L = 5.0 %, S_T = 2.5 %)

Part	$\boldsymbol{Q_{apr,i}}$ **[l/s]** (Lab / Num)	$\boldsymbol{Q_{Ii}}$ **[l/s]** (Lab / Num)
4+8	2.82 / 2.51	2.61 / 2.26
3+7	3.27 / 2.94	2.89 / 2.75
2+6	1.86 / 1.86	2.19 / 1.91
1+5	0.72 / 0.71	0.62 / 1.08

4. CONCLUSION

In order to develop new design approaches in urban drainage engineering several simulation runs were performed to improve planning tools, especially bidirectional coupled models which consider the interaction between the underground drainage system and the surface runoff. The connecting elements between both systems are street inlets which exist in different types and geometries. The present paper focuses on the hydraulic efficiency of a typical grate inlet used in Germany (500 mm x 500 mm) and its flow conditions in detail by locating and describing the main inflow areas of the grate and their corresponding efficiencies. In order to calibrate and validate a numerical model to calculate the efficiency of street inlets, physical model results were compared to three-dimensional numerical model results. With water depths up to 3 cm upstream of the inlet and flow velocities of 1-2 m/s only supercritical flow conditions occur due to steep longitudinal slopes up to S_L = 10 %. Depending on the investigated longitudinal and transverse slopes of the street, approximately 75 % of the approaching surface flow is captured by the inlet. The front half of the inlet intercepts nearly 70 % up to 95 % of the captured surface flow. The main inflow zone is on the front curbside zone which can be seen in both the physical and the numerical model. In order to validate the ability of the numerical model further research is necessary.

5. REFERENCES

Butler, D., Davies, J.W. (2011). Urban Drainage, Third Edition, Spon Press.

Brown, S.A., Schall, J.D., Morris, J.L., Doherty, C.L., Stein, S.M., and Warner, J.C. (2009). Urban Drainage Design Manual – Hydraulic Engineering Circular 22 (HEC-22), Third Edition, FHWA-NHI-10-009, U.S. Dept. of Transportation, Federal Highway Administration, Washington, D.C., National Highway Institute, Virginia.

Digman, C., Ashley, R., Hargreaves, P., and Gill, E. (2014). Managing urban flooding from heavy rainfall – encouraging the uptake of designing for exceedance. Recommendations and summary. CIRIA, London.

Despotovic, J., Plavsic, J., Stefanovic, N., and Pavlovic, D. (2005). Inefficiency of storm water inlets as a source of urban floods. *Water Science and Technology*, 51(2), 139-145.

DIN 19583 (2012). Gully tops 500 x 500 for road gullies, class C 250 and class D 400 – Part 2: Particulars. DIN Deutsches Institut für Normung e. V., Beuth Verlag GmbH, Berlin, Germany (in German).

DIN EN 752 (2008). Drain and sewer systems outside buildings; German version. DIN Deutsches Institut für Normung e. V., Beuth Verlag GmbH, Berlin, Germany (in German).

Djordjevic, S., Saul, A.J., Tabor, G.R., Blanksby, J., Galambos, I., Sabtu, N., and Sailor, G. (2013). Experimental and numerical investigation of interactions between above and below ground drainage systems. *Water Science and Technology*, 67(3), 535-542.

FGSV (2005). Richtlinie für die Anlage von Straßen – Teil Entwässerung (RAS-Ew). Ausgabe 2005. Forschungsgesellschaft für Straßen- und Verkehrswesen e. V., Cologne, Germany (in German).

Flow Science Inc. (editor) (2015). FLOW-3D User's manual. Version 11.1.

Fratini, C.F., Geldof, G.D., Kluck, J., and Mikkelsen, P.S. (2012). Three Points Approach (3PA) for urban flood risk management: A tool to support climate change adaption through transdisciplinarity and multifunctionality. *Urban Water Journal*, 9(5), 317-331.

Gómez, M., and Russo, B. (2005). Comparative study of methodologies to determine inlet efficiency from test data. HEC-12 methodology vs UPC method. Water Resource Management 2005, Algarve, Portugal.

Gómez, M., and Russo, B. (2007). Hydraulic efficiency of macro-inlets. *Proc. NOVATECH 2007*, 1157-1164

Gómez, M., and Russo, B. (2009). Hydraulic Efficiency of Continuous Transverse Grates for Paved Areas. *Journal of Irrigation and Drainage Engineering*. 135(2), 225-230.

Guo, J.C.Y., and MackKenzie, K. (2012). Hydraulic efficiency of grate and curb-opening inlets under clogging effect. Report No. CDOT-2012-3, Final Report. Colorado Department of Transportation, Denver.

IPCC (2014). Climate Change 2014: Synthesis Report. Contribution of Working Groups I, II and III to the Fifth Assessment Report of the Intergovernmental Panel on Climate Change [Core Writing Team, R.K. Pachauri and L.A. Meyer (eds)]. IPCC, Geneva, Switzerland.

Izzard, C.F. (1946). Hydraulics of runoff from developed surfaces. *Highway Res. Board Proc.* 26, 129-150.

Kemper, S. and Schlenkhoff, A. (2015). Determination of the hydraulic efficiency of intake structures like grate inlets and screens in supercritical flow. E-proceedings of the 36th IAHR World Congress, the Hague, the Netherlands.

KOSTRA-DWD-2000 (2000). Heavy precipitation totals in Germany (1951-2000). Deutscher Wetterdienst, Offenbach, Germany.

Lopes, P., Leandro, J., Carvalho, R.F., Russo, B., and Gómez, M. (2016). Assessment of the Ability of a Volume of fluid Model to Reproduce the Efficiency of a Continuous Transverse Gully with Grate. *Journal of Irrigation and Drainage Engineering*, 142(10).

Russo, B., Gómez, M., and Tellez, J. (2013). Methodology to Estimate the Hydraulic Efficiency of Nontested Continuous Transverse Grates. *Journal of Irrigation and Drainage Engineering*. 139(10), 864-871.

Spaliviero, F., May, R.W.P., and Excaramela, M. (2000). Spacing of Road Gullies – Hydraulic performance of BS EN 124 gully gratings and kerb inlets. Report SR 533, HR Wallingford.